

Recombinant expression, purification and crystallographic studies of the mature form of human mitochondrial aspartate aminotransferase

Xiuping Jiang^{1,*}, Jia Wang¹, Haiyang Chang¹, Yong Zhou²

¹ School of Life Science and Biotechnology, Dalian University of Technology, Dalian 116024, China;

² School of Software, Dalian University of Technology, Dalian 116620, China.

Summary

Mitochondrial aspartate aminotransferase (mAspAT) was recognized as a moonlighting enzyme because it has not only aminotransferase activity but also a high-affinity long-chain fatty acids (LCFA) binding site. This enzyme plays a key role in amino acid metabolism, biosynthesis of kynurenic acid and transport of the LCFA. Therefore, it is important to study the structure-function relationships of human mAspAT protein. In this work, the mature form of human mAspAT was expressed to a high level in *Escherichia coli* periplasmic space using pET-22b vector, purified by a combination of immobilized metal-affinity chromatography and cation exchange chromatography. Optimal activity of the enzyme occurred at a temperature of 47.5°C and a pH of 8.5. Crystals of human mAspAT were grown using the hanging-drop vapour diffusion method at 277K with 0.1 M HEPES pH 6.8 and 25%(v/v) Jeffamine[®] ED-2001 pH 6.8. The crystals diffracted to 2.99 Å and belonged to the space group *P1* with the unit-cell parameters $a = 56.7$, $b = 76.1$, $c = 94.2$ Å, $\alpha = 78.0$, $\beta = 85.6$, $\gamma = 78.4^\circ$. Elucidation of mAspAT structure can provide a molecular basis towards understanding catalysis mechanism and substrate binding site of enzyme.

Keywords: Aspartate aminotransferase (AspAT), plasma membrane fatty acid binding protein (FABPpm), kynurenine aminotransferase-IV, crystallization, moonlighting protein

1. Introduction

Aspartate aminotransferase (AspAT, EC 2.6.1.1) is present as two homologous, genetically independent isozymes in animal cells, one located in the cytoplasm (cAspAT) and the other in mitochondria (mAspAT) (1,2). mAspAT was recognized as a moonlighting enzyme because it was found to have two or more different functions. Similar to cAspAT, mAspAT catalyzes the reversible reaction of L-aspartate and α -ketoglutarate (α -KG) into oxaloacetate and L-glutamate via a ping-pong mechanism, with pyridoxal 5'-phosphate (PLP) as an essential cofactor (3). Glutamine not only provides a

carbon source to fuel the tricarboxylic acid (TCA) cycle via α -KG, but also provides nitrogen for the synthesis of nonessential amino acids and nucleotides, *i.e.*, purines, pyrimidines, alanine, serine, aspartate, ornithine, glycine, cysteine, arginine, asparagine, and proline (4,5). Therefore, mAspAT is one of the key enzymes that links amino acid metabolism to carbohydrate metabolism through catalysis of the reversible transamination reaction.

Different to cAspAT, mammalian mAspAT is also recognized as kynurenine aminotransferase-IV because this enzyme is capable of catalyzing the irreversible transamination of kynurenine to produce kynurenic acid (KYNA) and plays a role in the biosynthesis of KYNA in rat, mouse and human brains (6-8). KYNA is an endogenous antagonist of *N*-methyl-D-aspartate and α 7-nicotinic acetylcholine receptors (9,10). In addition, KYNA is identified as an endogenous ligand for an orphan G-protein-coupled receptor (11). Abnormal concentration of KYNA in brain tissue has been observed in patients with mental and neurological disorders,

Released online in J-STAGE as advance publication February 22, 2016.

*Address correspondence to:

Dr. Xiuping Jiang, School of Life Science and Biotechnology, Dalian University of Technology, Linggong Road No.2, Dalian116024, China.

E-mail: xpjiang@dlut.edu.cn

including the Huntington's disease, Alzheimer's disease, and schizophrenia (12). Therefore, mAspAT can be envisioned to be a valid molecular target for the treatment of these neurological diseases.

Additionally, mAspAT is recognized as plasma membrane fatty acid binding protein (FABP_{pm}) because this enzyme has a high affinity for long-chain fatty acids (LCFA) and is a key enzyme involved in the transport of the saturated LCFA and unsaturated LCFA (13,14). Accordingly, it is important to study the structure-function relationships of mAspAT protein because it possesses both enzymatic catalytic activity and LCFA binding activity. To date, AspATs have been purified from many sources and X-ray structures have been determined for those from *Escherichia coli* (15), cytosolic yeast cytoplasm (16), pig cytoplasm (17), chicken mitochondria (18), and chicken cytoplasm (19). However, the crystal structure of the human mAspAT has not been solved.

Human mAspAT contains 4 cysteine residues forming two disulfide bonds. In addition, the overexpression of mAspAT is toxic to the growth of host cells as mAspAT is a key metabolic enzyme in amino acid metabolism. This study aimed to generate and purify recombinant human mAspAT protein in a high level that is sufficient for characterization analysis and further structural studies. We report here the expression, purification and characterization of human mAspAT expression in *E. coli* periplasmic space using the plasmid pET-22b. Moreover, the crystallization and preliminary X-ray analysis of mAspAT protein were also performed.

2. Materials and Methods

2.1. Materials

The pET-22b (+) vector and *E. coli* strain BL21 (DE3) were obtained from Novagen (Beijing, China). pMD18-T Simple Vector, *E. coli* strain JM 109, T4 DNA ligase, *Ex* Taq DNA polymerase, *Nco* I and *Xho* I restriction enzymes were purchased from Takara Biotechnology (Dalian, China). The Amicon Ultra centrifugal filter (3 kDa) used for filtration of the cell culture medium was obtained from Millipore Corporation (Bedford, MA, USA). The AST (SGOT) Reagent Kit used for monitoring the activity of mAspAT was purchased from BIO QUANT (San Diego, CA, USA). Crystallization Screening kits were purchased from Hampton Research (Oklahoma City, OK, USA). All primers were synthesized by Takara Biotechnology.

2.2. Construct of expression vector

The nucleotide sequence encoding for the mature form of human mAspAT (GenBank accession no. M22632.1) was artificially synthesized by Taihe Biotechnology

Co., Ltd. (Beijing, China). *Nco* I and *Xho* I restriction sites were added to the N-terminus and C-terminus of the mAspAT sequence by PCR, respectively, using the forward primer F1 5'-CATGCCATGGCAGAGCCAG CTCCTGGTGGGA-3' (*Nco* I site is underlined) and the reverse primer R1 5'-CCGCTCGAGCTTGGTGACCT GGTGAATGGCAT-3' (*Xho* I is underlined). The PCR product was digested with *Nco* I-*Xho* I, and cloned into the *Nco* I-*Xho* I site of the pMD18-T simple vector and then transformed into *E. coli* strain JM 109. Nucleic acid sequences of the cloning DNA fragment were confirmed by DNA sequencing (BigDye™ Kit, Applied Biosystems, USA) and ABI PRISM™ 3730XL DNA Analyzer, according to the recommended protocols. The target DNA fragment was further subcloned in the same site of pET-22b (+) vector, resulting in pET22b-hmAspAT. The resulting vector was then transformed into chemically competent *E. coli* strain BL21 (DE3) by heat shock for protein expression.

2.3. Expression of human mAspAT

The single colony of *E. coli* BL21 (DE3) harboring the expression vector in 30 mL of Luria-Bertani (LB) medium containing 100 µg/mL ampicillin, and then cultivated at 37°C until the optical density (OD₆₀₀) reached 0.6. The cells were harvested by centrifugation at 4,000 × g for 10 min, and resuspended in 3 L fresh LB medium containing 100 µg/mL ampicillin. Subsequently, protein expression was induced with 1 mM isopropyl β-D-1-thiogalactopyranoside (IPTG) for 20 h at 16°C. The cells were harvested by centrifugation at 8,000 × g for 15 min and washed with buffer A (20 mM NaH₂PO₄, 0.5 M NaCl, pH 7.4). Approximated 45 g (wet weight) cells were obtained from 3 L culture. After centrifugation, the cell pellets was resuspended in 40 mL (for 1 L culture) ice-cold extraction buffer A, and lysed by ultrasonication at ice-cold temperature using an UP400S instrument (Dr. Hielscher GmbH, Stuttgart, Germany). The cell lysis was centrifuged at 12,000 rpm for 15 min to separate soluble (supernatant) and precipitated (pellet) fractions.

2.4. Purification of human mAspAT

The resulting supernatant was filtered with a 0.22 µm syringe filter and then loaded onto a 5 mL HisTrap™ FF crude column (GE Healthcare, Uppsala, Sweden) pre-equilibrated with buffer A. After washing the column with buffer A containing 50 mM imidazole, the target protein was eluted with buffer B (20 mM NaH₂PO₄, 0.5 M NaCl, 300 mM imidazole, pH 7.4). The buffer was exchanged with 20 mM Tris buffer (pH 7.5) containing 20 mM NaCl using a 5 mL HiTrap™ desalting column (GE Healthcare). The desalted sample was loaded onto a 1 mL SP Sepharose™ FF column (GE Healthcare). After washing, the column

was eluted with a linear gradient of NaCl from 20 to 500 mM in Tris buffer (pH 7.5) at a flow rate of 1 mL/min. Fractions with enzyme activity were pooled and the buffer was exchanged for 20 mM Tris (pH 7.0) containing 20 mM NaCl by using a 5 mL HiTrapTM desalting column (GE Healthcare), and then the protein was concentrated to a final concentration of 5 mg/mL with a 3 kDa cut-off concentrator (Millipore). During purification, the activity of mAspAT was monitored using the AST (SGOT) Reagent Kit (BQ Kits). In this method, a diazonium salt was used which selectively reacted with the oxalacetate to produce a color complex that was measured photometrically. According to the protocol, reaction mixture including enzyme, substrate, assay buffer and assay developer was incubated at 37°C for 60 min, and OD₄₅₀ was then measured. One unit of enzyme is defined as the amount of enzyme which generates 1.0 μmol of glutamate per minute at 37°C. The purity of the eluted protein was analyzed by SDS-PAGE and found to be > 95%.

2.5. SDS-PAGE and Western blot analysis

SDS-PAGE analysis was performed using 12% resolving gel and 5% stacking gel. The protein bands were visualized by Coomassie brilliant blue R-250 and then analyzed by image-density analysis software (Gel-Pro, USA). Soluble fractions of cell lysates after IPTG induction were subjected to SDS-PAGE and transferred to polyvinylidene difluoridemembrane (Millipore). The membranes were blocked with 5% defatted milk at room temperature for 60 min and then incubated with anti-his tag mouse monoclonal antibody (1 μg/mL, Millipore) at 4°C overnight. The membranes were washed twice with PBS buffer and incubated with horseradish peroxidase conjugated goat anti-mouse IgG (1:5,000, Millipore) at room temperature for 90 min. Finally, the membranes were washed five times with PBS buffer, and a 3'-diaminobenzidine kit was used for color development (Sigma-Aldrich, St. Louis, Mo, USA).

2.6. Crystallization and X-ray diffraction of human mAspAT

Initial crystallization screening was carried out in 24-well tissue-culture plates at 277 K by the hanging-drop vapor diffusion method using commercially available Index Screen, Crystal Screen, Crystal Screen 2 and PEG/Ion Screen (Hampton Research). Crystals were grown in a mixture containing 1 μL of protein (5 mg/mL in 20 mM Tris pH 7.0, 20 mM NaCl) and 1 μL of reservoir solution and were equilibrated against 400 μL reservoir solution. Crystallization conditions were optimized based on the initial screening.

Single crystals were soaked for several minutes in a reservoir solution containing 25%(v/v) glycerol and

were then flash-cooled in liquid nitrogen. All X-ray diffraction data were collected on the ESRF beamline BL-17U at the Shanghai Synchrotron Radiation Facility in China and were processed using the HKL-2000 package (20). Diffraction data were collected at a wavelength of 0.98 Å, an oscillation angle of 1°, an exposure time of 1 s per image and a crystal-to-detector distance of 250 mm.

3. Results and Discussion

Human mAspAT is encoded by nuclear gene and synthesized in the cytoplasm as precursor protein containing N-terminal presequences of 30 amino acid residues in length (21). After completion of translation, human mAspAT is imported into mitochondria matrix *via* several apparently discrete steps including proteolytic cleavage of the presequence with processing proteases and assembly into mature protein (22,23). Therefore, the mature form of human is post-translationally imported into the mitochondrial matrix and lack 30 amino acid residues from the N-terminus compared with the precursor (24). The recombinant expression results indicated that the precursor form of mAspAT was found to express as inclusion body in *E. coli* expression system, however, the mature could be found in the supernatant of the bacterial homogenate (25). Therefore the mature form of human mAspAT was chosen to study the recombinant expression and crystallization of protein.

Human mAspAT is a toxic protein to host cell and also contains 4 cysteine residues forming two disulphide bonds. In order to obtain the large amounts of soluble mature mAspAT in *E. coli* for the crystallization study, we introduced the use of pET-22b plasmid as the expression vector. The pET-22b vector possessed an N-terminal *pelB* secretion signal under the control of the strong bacteriophage T7 promoter, which directed the recombinant protein to the *E. coli* periplasmic space (26). The periplasm of *E. coli* contains the disulfide oxidoreductases and isomerases, which is an oxidizing environment and can facilitate formation of disulfide bonds that are always required for correct protein folding (27,28). Therefore the periplasm of *E. coli* was expected to be an ideal compartment for expression of human mAspAT.

The plasmid pET22b- hmAspAT was then transformed into *E. coli* BL21 (DE3). When the culture was propagated at 37°C until OD₆₀₀ reached 0.6, the expression of the fusion protein was induced with 1.0 mM of IPTG, and then the culture was grown for an additional 20 h at 16°C. After lysis, the supernatant was analyzed by Western blotting using anti-his tag mouse antibody. Western blot analysis confirmed that the recombinant human mAspAT was present in the soluble fraction of the cell lysate after induction with IPTG (Figure 1A).

Recombinant human mAspAT was purified by a combination of immobilized metal-affinity chromatography and cation exchange chromatography. The purified protein was resolved as a single band in the SDS-PAGE gel with a molecular mass of about 43 kDa, indicating that these two chromatographic steps were very effective (Figure 1B, lane 3). The final yield of pure protein was approximately 10 mg from 1 L of expression culture, allowing the preparation of approximately 2 mL of a 5.0 mg/mL protein sample for crystallization assays. After two chromatography steps, the specific activity and overall recovery of purified mAspAT were 36.3 U/mg and 19.4%, respectively (Table 1). The purification of mAspAT protein is

summarized in Table 1.

The optimal pH for enzyme activity was determined to be pH 8.5 (Figure 2A), similar to that (pH 8.0) of AspAT from *Bacillus subtilis* (29). Actually, the enzyme activity over the pH range 8.0-10.0 was more than 60% of the maximum activity (Figure 2A). Moreover, human mAspAT showed optimal activity at 47.5°C and maintained over 80% activity at temperatures from 40 to 60°C, indicating a certain degree of thermostability in this temperature range (Figure 2B). The recombinant human mAspAT tended to have relatively high activity and stability in alkaline environments, similar to that of the AspATs from *B. subtilis* and *B. circulans* (29,30). Thus the recombinant human mAspAT had optimal

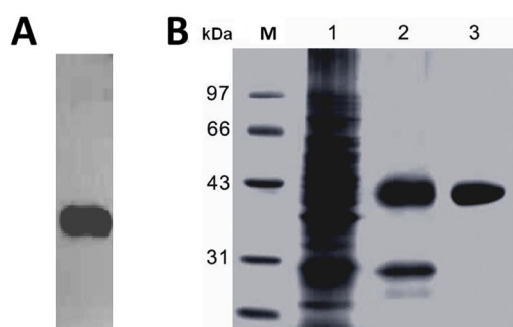


Figure 1. Quality assessment of human mAspAT expression and purification. (A) Western blot analysis of human mAspAT expression using an anti-his tag mouse monoclonal antibody. Lane 1, soluble fraction of the cell lysate after induction with IPTG. (B) SDS-PAGE analysis of human mAspAT samples during protein purification. Lane M, protein marker; lane 1, soluble fraction after cell lysis; lane 2, elution fractions from the HisTrap™ FF crude column; lane 3, elution fractions from the SP Sepharose™ FF column.

Table 1. Purification efficiency of recombinant human mAspAT

Purification step	Specific activity (U/mg)	Purification (fold)	Yield (%)
Lysate supernatant	0.574	1	100
His Trap	12.5	8.42	21.9
SP Sepharose	36.3	26.8	19.4

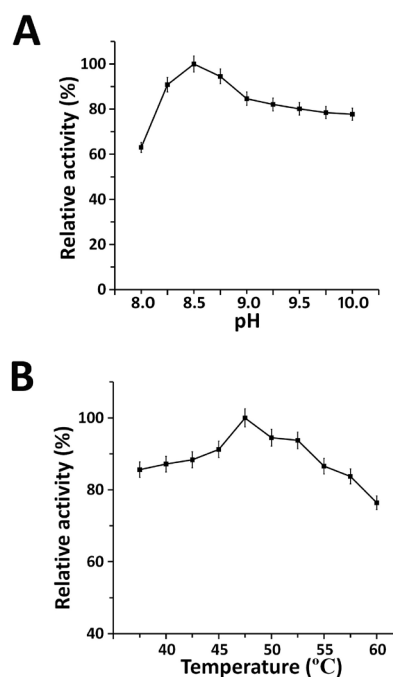


Figure 2. Effects of pH and temperature on activity of purified recombinant human mAspAT. Enzyme activity was determined at different pHs (A) and temperatures (B) using the AST (SGOT) Reagent Kit.

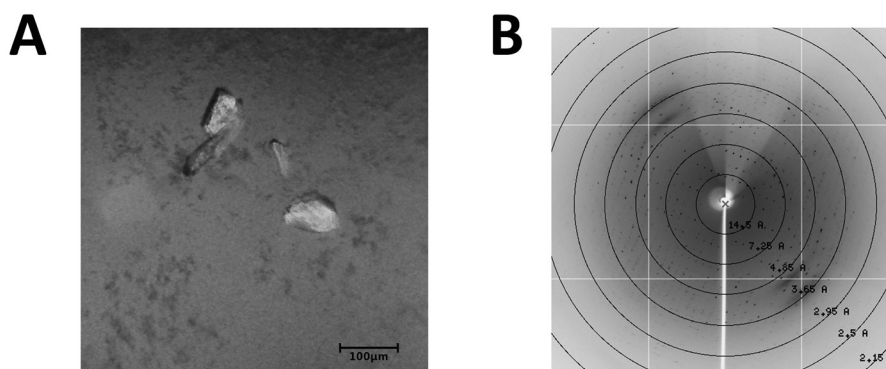


Figure 3. Crystals and X-ray diffraction image of recombinant human mAspAT. (A) Crystals grown in 0.1 M HEPES pH 6.8 and 25%(v/v) Jeffamine® ED-2001 pH 6.8 at 277 K. (B) X-ray diffraction image of human mAspAT.

Table 2. Data collection and processing

Diffraction source	BL-17U, ESRF
Wavelength (Å)	0.98
Temperature (K)	100
Crystal-detector distance (mm)	250
Rotation range per image (°)	1
Total rotation range (°)	180
Exposure time per image (s)	1
Space group	<i>P1</i>
<i>a</i> , <i>b</i> , <i>c</i> (Å)	56.7, 76.1, 94.2
α , β , γ (°)	78.0, 85.6, 78.4
Resolution range (Å)	2.99
Total No. of reflections	578579
No. of unique reflections	30161
Completeness (%)	97.2 (97.1)
Average <i>I</i> / σ (<i>I</i>)	4.3 (2.0)
<i>R</i> _{merge} (%)*	0.083 (0.265)
<i>R</i> _{meas} (%)**	0.117 (0.375)

* $R_{\text{merge}} = \frac{\sum_{hkl} \sum_i |I_i(hkl) - \langle I(hkl) \rangle|}{\sum_{hkl} \sum_i I_i(hkl)}$.

** $R_{\text{meas}} = \frac{\sum_{hkl} \{N(hkl) / [N(hkl)-1]\}^{1/2} \sum_i |I_i(hkl) - \langle I(hkl) \rangle|}{\sum_{hkl} \sum_i I_i(hkl)}$, where $\langle I(hkl) \rangle$ is the mean intensity of the *N*(*hkl*) observations *I*(*hkl*) of each unique reflection *hkl* after scaling.

activity at pH 8.5 and 47.5°C.

Initial crystallization screening yielded a crystallization hit under the condition No. 39 of the Index Screen consisting of 0.1 M HEPES pH 7.0 and 30%(v/v) Jeffamine[®] ED-2001 pH 7.0. This condition was subsequently optimized by testing 231 new crystallization combinations with varying pH values from 6.5 to 7.5 using HEPES buffer and Jeffamine[®] ED-2001 concentrations from 20 to 40%(v/v). Finally, we obtained an optimal composition for the reservoir solution of 0.1 M HEPES pH 6.8 and 25%(v/v) Jeffamine[®] ED-2001 pH 6.8 (Figure 3A).

The human mAspAT crystal data were collected to a resolution of 2.99 Å (Figure 3B) and processed using the HKL-2000 package (20). The crystals belonged to the space group *P1*, with unit cell parameters *a* = 56.7, *b* = 76.1, *c* = 94.2 Å, α = 78.0, β = 85.6, and γ = 78.4°. The space group of cytosolic AspATs from chicken (19), pig heart (17), and *Saccharomyces cerevisiae* (16) is *P2₁2₁2₁*, while the space group for AspAT crystals from *E. coli* is *P2₁* (15). Data collection statistics are summarized in Table 2.

In conclusion, we constructed the expression construct for human mAspAT and expressed it as an active enzyme in *E. coli* periplasmic space. Moreover, the recombinant human mAspAT was purified and its some biochemical properties were also examined. The crystals of mAspAT protein have been obtained by the hanging-drop vapor-diffusion method and an X-ray diffraction data set was collected from a single crystal to 2.99 Å resolution. This study may provide a method useful for the recombinant preparation of other cytotoxic proteins. The structure of mAspAT protein will provide insight into the structure reactivity relationships of human mAspAT and its substrates. The human mAspAT structure will be useful for screening

of its inhibitors and may also have implications for future therapeutic approaches.

Acknowledgements

This study was supported by grants from the National Natural Science Foundation of China (81102378, 61202252) and from the Specialized Research Fund for the Doctoral Program of Higher Education of China (20120041120052).

References

- Boyd JW. The intracellular distribution, latency and electrophoretic mobility of L-glutamate-oxaloacetate transaminase from rat liver. *Biochem J.* 1961; 81:431-441.
- Katsunuma N, Matsuzawa T, Fujino A. Differences between the transaminases in mitochondria and soluble fraction. II. Glutamic-oxaloacetic transaminase. *J Vitaminol (Kyoto).* 1962; 8:74-79.
- Toney MD. Aspartate aminotransferase: An old dog teaches new tricks. *Arch Biochem Biophys.* 2014; 544:119-127.
- Young VR, Ajami AM. Glutamine: The emperor or his clothes? *J Nutr.* 2001; 131:2449S-2459S.
- DeBerardinis RJ, Mancuso A, Daikhin E, Nissim I, Yudkoff M, Wehrli S, Thompson CB. Beyond aerobic glycolysis: Transformed cells can engage in glutamine metabolism that exceeds the requirement for protein and nucleotide synthesis. *Proc Natl Acad Sci U S A.* 2007; 104:19345-19350.
- Guidetti P, Amori L, Sapko MT, Okuno E, Schwarcz R. Mitochondrial aspartate aminotransferase: A third kynurenate-producing enzyme in the mammalian brain. *J Neurochem.* 2007; 102:103-111.
- Han Q, Cai T, Taqle DA, Li J. Structure, expression, and function of kynurenine aminotransferases in human and rodent brains. *Cell Mol Life Sci* 2010; 67:353-368.
- Han Q, Robinson H, Cai T, Taqle DA, Li J. Biochemical and structural characterization of mouse mitochondrial aspartate aminotransferase, a newly identified kynurenine aminotransferase-IV. *Biosci Rep.* 2011; 31:323-332.
- Foster AC, Kemp JA, Leeson PD, Grimwood S, Donald AE, Marshall GR, Priestley T, Smith JD, Carling RW. Kynurenic acid analogues with improved affinity and selectivity for the glycine site on the *N*-methyl-D-aspartate receptor from rat brain. *Mol Pharmacol.* 1992; 41:914-922.
- Beggiato S, Antonelli T, Tomasini MC, Tanganelli S, Fuxe K, Schwarcz R, Ferraro L. Kynurenic acid, by targeting $\alpha 7$ nicotinic acetylcholine receptors, modulates extracellular GABA levels in the rat striatum *in vivo*. *Eur J Neurosci.* 2013; 37:1470-1477.
- Wang J, Simonavicius N, Swaminath G, Reagan J, Tian H, Ling L. Kynurenic acid as a ligand for orphan G protein-coupled receptor GPR35. *J Biol Chem.* 2006; 281:22021-22028.
- Németh H, Toldi J, Vécsei L. Kynurenines, Parkinson's disease and other neurodegenerative disorders: Preclinical and clinical studies. *J Neural Transm Suppl.* 2006; 70:285-304.
- Bradburry MW, Stump D, Guarnieri F, Berk PD.

- Molecular modeling and functional confirmation of a predicted fatty acid binding site of mitochondrial aspartate aminotransferase. *J Mol Biol.* 2011; 412:421-422.
14. Roepstorff C, Helge JW, Visitisen B, Kiens B. Studies of plasma membrane fatty acid-binding protein and other lipid-binding proteins in human skeletal muscle. *Pro Nutr Soc.* 2004; 63:239-244.
 15. Jäger J, Moser M, Sauder U, Jansonius JN. Crystal structures of *Escherichia coli* aspartate aminotransferase in two conformations. Comparison of an unliganded open and two liganded closed forms. *J Mol Biol.* 1994; 239:285-305.
 16. Jeffery CJ, Barry T, Doonan S, Petsko GA, Ringe D. Crystal structure of *Saccharomyces cerevisiae* cytosolic aspartate aminotransferase. *Protein Sci.* 1998; 7:1380-1387.
 17. Rhee S, Silva MM, Hyde CC, Rogers PH, Metzler CM, Metzler DE, Arnone A. Refinement and comparisons of the crystal structures of pig cytosolic aspartate aminotransferase and its complex with 2-methylaspartate. *J Biol Chem.* 1997; 272:17293-17302.
 18. Ford GC, Eichele G, Jansonius JN. Three-dimensional structure of a pyridoxal-phosphate-dependent enzyme, mitochondrial aspartate aminotransferase. *Proc Natl Acad Sci U S A.* 1980; 77:2559-2563.
 19. Malashkevich VN, Strokopytov BV, Borisov VV, Dauter Z, Wilson KS, Torchinsky YM. Crystal structure of the closed form of chicken cytosolic aspartate aminotransferase at 1.9 Å resolution. *J Mol Biol.* 1995; 247:111-124.
 20. Otwinowski Z, Minor W. Processing of x-ray diffraction data collected in oscillation mode. *Methods Enzymol.* 1997; 276:307-326.
 21. Nishi T, Nagashima F, Tanase S, Fukumoto Y, Joh T, Shimada K, Matsukado Y, Ushio Y, Morino Y. Import and processing of precursor to mitochondrial aspartate aminotransferase. Structure-function relationships of the presequence. *J Biol Chem.* 1989; 264:6044-6051.
 22. Warren G. Protein transport. Signals and salvage sequences. *Nature.* 1987; 327:17-18.
 23. Lain B, Yañez A, Iriarte A, Martinez-Carrion M. Aminotransferase variants as probes for the role of the N-terminal region of a mature protein in mitochondrial precursor import and processing. *J Biol Chem.* 1998; 273:4406-4415.
 24. Sonderegger P, Jaussi R, Christen P. Cell-free synthesis of a putative precursor of mitochondrial aspartate aminotransferase with higher molecular weight. *Biochem Biophys Res Commun.* 1980; 94:1256-1260.
 25. Jaussi R, Behra R, Giannattasio S, Flura T, Christen P. Expression of cDNAs encoding the precursor and the mature form of chicken mitochondrial aspartate aminotransferase in *Escherichia coli*. *J Biol Chem.* 1987; 262:12434-12437.
 26. Yoon SH, Kim SK, Kim JF. Secretory production of recombinant proteins in *Escherichia coli*. *Recent Pat Biotechnol.* 2010; 4:23-29.
 27. De Marco A. Strategies for successful recombinant expression of disulfide bond-dependent proteins in *Escherichia coli*. *Microb Cell Fact.* 2009; 8:26.
 28. Berkmen M. Production of disulfide-bonded proteins in *Escherichia coli*. *Protein Expr Purif.* 2012; 82:240-251.
 29. Wu HJ, Yang Y, Wang S, Qiao JQ, Xia YF, Wang Y, Wang WD, Gao SF, Liu J, Xue PQ, Gao XW. Cloning, expression and characterization of a new aspartate aminotransferase from *Bacillus subtilis* B3, *FEBS J.* 2011; 278:1345-13457.
 30. Kravchuk Z, Tsybovsky Y, Koivulehto M, Chumanevich A, Battchikova N, Martsev S, Korpela T. Truncated aspartate aminotransferase from alkalophilic *Bacillus circulans* with deletion of N-terminal 32 amino acids is a non-functional monomer in a partially structured state. *Protein Eng.* 2001; 14:279-285.

(Received November 6, 2015; Revised February 9, 2016; Accepted February 11, 2016)